# Supporting Information

Zhao et al. 10.1073/pnas.1306699110

## SI Text

**Analysis of FRET Efficiencies Reflected in Measured FRET Ratios.** In the presence of a given fluorescence resonance energy transfer (FRET) efficiency $F$ excitation of CFP produces a fluorescence intensity $I_C$ in the CFP channel:

$$I_C = f_{CC} \cdot S \cdot (1-F). \quad \text{[S1]}$$

The constant factor $f_{CC}$ includes CFP excitation efficiency, the emission efficiency of CFP in the CFP detection band, and the light collection efficiency in this band. $S$ is the density of SNARE COmplex REporter (SCORE) in the membrane.

The fluorescence intensity in the YFP (Venus) channel $I_Y$ is the sum of three contributions (1):

*i*) CFP emission in the YFP channel:

$$I_{CY} = f_{CY} \cdot S \cdot (1-F). \quad \text{[S2]}$$

The factor $f_{CY}$ includes CFP excitation efficiency, the emission efficiency of CFP in the YFP detection band, and the light collection efficiency in this band.

*ii*) YFP emission in the YFP channel due to FRET:

$$I_Y = f_{YY,FRET} \cdot S \cdot F. \quad \text{[S3]}$$

The factor $f_{YY,FRET}$ includes CFP excitation efficiency, the emission efficiency of YFP in the YFP detection band, and the light collection efficiency in this band.

*iii*) YFP emission in the YFP channel due to direct excitation of YFP with 436-nm light:

$$I_Y = f_{YY,DIRECT} \cdot S. \quad \text{[S4]}$$

The factor $f_{YY,DIRECT}$ includes YFP excitation efficiency, the emission efficiency of YFP in the YFP detection band, and the light collection efficiency in this band.

The measured intensity ratio $R$ can thus be expressed as

$$R = \frac{I_Y}{I_C} = \frac{f_{CY}}{f_{CC}} + \frac{f_{YY,DIRECT}}{f_{CC}} + \left(\frac{f_{YY,FRET}}{f_{CC}} + \frac{f_{YY,DIRECT}}{f_{CC}}\right) \cdot \frac{F}{1-F}. \quad \text{[S5]}$$

The ratio $f_{CY}/f_{CC}$ was measured in cells expressing CFP-tagged SNAP25 to be 0.42. The ratio $f_{YY,DIRECT}/f_{CC}$ was estimated based on the spectroscopic properties of CFP and Venus and the transmission curves of the filters to be ~0.22.

Eq. **S5** can be written in simplified form as

$$R = \frac{I_Y}{I_C} = A + B \cdot \frac{F}{1-F} \quad \text{[S6]}$$

with the coefficient $A = \frac{f_{CY}}{f_{CC}} + \frac{f_{YY,DIRECT}}{f_{CC}} \sim 0.64$.

The coefficient $B$ can be estimated based on an acceptor photobleaching experiment of SCORE expressed in live chromaffin cells (Fig. S3). SCORE was excited in total internal reflection (TIR) mode through a 436/10-nm excitation filter and a CFP/YFP dual-band beam splitter (51017bs; Chroma) instead of the 455-nm dichroic. The fluorescence image was separated into CFP and Venus components as in the other experiments. Images were acquired every 1 s with 200-ms exposure time. Between exposures, excitation was switched to a 508/20-nm filter using a filter wheel and the TIR annulus switched out using a second filter wheel. The filter wheels were controlled through a Lambda 10-2 controller (Sutter Instrument Company) by the software of the EMCCD camera (iXon; Andor). The acceptor photobleaching led to a decrease in YFP fluorescence $I_Y$ and a concomitant increase in CFP fluorescence intensity $I_C$ (Fig. S3). Before acceptor photobleaching $I_C$ was 15% lower than after, correponding to an initial FRET efficiency of 0.15.

In the exocytosis measurements the mean baseline intensity ratio averaged over the cells' footprints was ~1.11. With the value $F = 0.15$ the coefficient $B$ is found to be 2.7. $B$ is dominated by the ratio $f_{YY,FRET}/f_{CC}$, which reflects the ratio of brightness at 100% FRET from YFP only to that at 0% FRET from CFP only. This ratio was also estimated based on the spectroscopic properties of CFP and YFP and the filter transmission curves to be 2.5, in good agreement with the determination based on acceptor photobleaching.

Solving Eq. **S6** for the FRET efficiency $F$ yields

$$F = \frac{(R-A)}{(B+R-A)}. \quad \text{[S7]}$$

Eq. **S7** can now be used to estimate the apparent FRET efficiencies. The baseline values at fusion sites ($R = 1.14$) gives $F = 0.158$ and the FRET efficiency during the transient FRET increase ($R = 1.21$) is $F = 0.176$.

**Estimate of Fractions of Molecules Contributing to Observed FRET Changes.** The above estimates were based on the assumption that all molecules measured in a given region show the same FRET efficiency and that all molecules at the fusion site undergo the same change. This, however, is not the case given the specific differences at fusion sites and changes during fusion events. We therefore ask how the data may be interpreted based on the assumption that SCORE may exist in two distinct conformations that show two different FRET efficiencies. If we assume that a fraction $\alpha$ of molecules exhibit high FRET efficiency ($F_{high}$) whereas the remaining molecules show low FRET efficiency ($F_{low}$), the intensities in the CFP and YFP channels become

$$I_C = (1-\alpha) \cdot f_{CC} \cdot S \cdot (1-F_{low}) + \alpha \cdot f_{CC} \cdot S \cdot (1-F_{high}) \quad \text{[S8]}$$

$$I_Y = \frac{f_{CY}}{f_{CC}} \cdot I_C + f_{YY,DIRECT} \cdot S + (1-\alpha) \cdot f_{YY,FRET} \cdot S \cdot F_{low} + \alpha \cdot f_{YY,FRET} \cdot S \cdot F_{high} \quad \text{[S9]}$$

and the fluorescence intensity ratio

$$R = \frac{I_Y}{I_C} = A + B \cdot \frac{F_{low} + \alpha \cdot (F_{high} - F_{low})}{1 - [F_{low} + \alpha \cdot (F_{high} - F_{low})]}. \quad \text{[S10]}$$

Comparing Eq. **S10** to Eq. **S6** reveals that the apparent FRET efficiencies in Eq. **S6** correspond to the expression $F_{app} = F_{low} + \alpha \cdot (F_{high} - F_{low})$ in Eq. **S9** and $\alpha$ can be calculated as

$$\alpha = \frac{F_{app} - F_{low}}{F_{high} - F_{low}}. \quad \text{[S11]}$$

In our experiments, overexpression of SCORE means that most of the SCORE will not be in a complex with syntaxin and

we therefore assign the average FRET ratio in the cells' footprints $R_{min}$ = 1.11 to the footprint FRET efficiency of 0.15 (Fig. S3) as $F_{low}$. In PC12 cells coexpressing SCORE and high amounts of syntaxin, the intensity ratio approached $R_{max}$ ~2.4 in measurements using similar filters (2). Using Eq. **S6** and the calibration values determined here, this corresponds to $F_{high}$ ~0.4.

For the $F_{app}$ values of 0.158 (baseline at fusion sites) and 0.176 during the transient FRET increase during fusion, this yields estimates for $\alpha$ of 0.03 and 0.1, respectively. These estimates suggest that ~3% of the SCORE molecules are in the high-FRET state at fusion sites and that a conformational change of ~7% of SCORE molecules from the low-FRET to the high-FRET state precedes fusion of a vesicle.

In PC12 cells endogenous SNAP25 is present at a density of ~7,500 molecules per μm$^2$. Based on immunofluorescence analysis SCORE was overexpressed in chromaffin cells at a level that is typically approximately sevenfold higher than endogenous SNAP25. If the SNAP25 density in chromaffin cells is similar to that in PC12 cells, this would correspond to ~50,000 SCORE molecules per μm$^2$. Here we analyze 0.1-μm$^2$ areas (four pixels) measuring fluorescence from ~5.000 copies of SCORE (although in fact partial fluorescence from a larger number is captured). These rough estimates suggest that on average in a four-pixel fusion site ~150 copies of SCORE are in the high-FRET state. When the FRET increase happens 90 ms before fusion, an additional 350 copies of SCORE make the transition from the low-FRET to the high-FRET state. The SNAP25 density in the plasma membrane of bovine chromaffin cells is currently unknown and the estimates of absolute SCORE copy numbers may thus not be correct. However, the data indicate that the observed local rapid FRET change preceding fusion may be due to a conformational change of ~7% of the molecules present near the fusion site but not elsewhere on the plasma membrane.


1. Erickson MG, Alseikhan BA, Peterson BZ, Yue DT (2001) Preassociation of calmodulin with voltage-gated Ca(2+) channels revealed by FRET in single living cells. *Neuron* 31(6):973–985.

2. An SJ, Almers W (2004) Tracking SNARE complex formation in live endocrine cells. *Science* 306(5698):1042–1046.


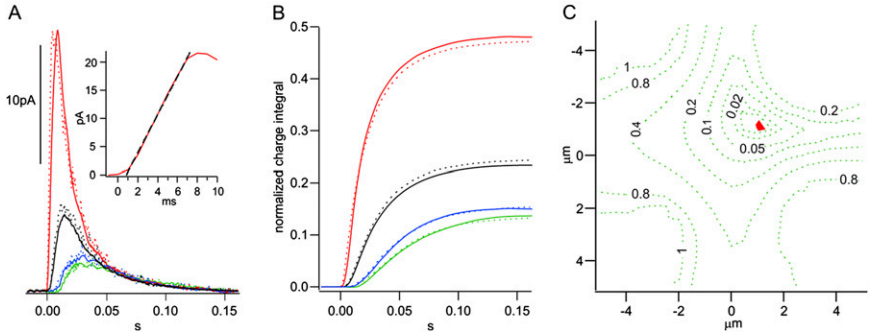


**Fig. S1.** Determination of vesicle release site and diffusional delays by random-walk simulation (RWS). (*A* and *B*) Time courses of the amperometric signals (*A*) and their charge integrals (*B*) of the fusion event of Fig. 1 *B*, *II* (solid lines). The dotted lines show the time course of the simulated signals for the best-fitting release site, marked with the red square in Fig. 1 *A*, *II*. For RWS, the distance between cell membrane and electrochemical detector (ECD) array surface is set to 0.1 μm and the diffusion coefficient fitted to 90 μm$^2$/s. Release is assumed to be instantaneous at time 0. The distance *r* between a release site and an electrode results in a 2D diffusion time $r^2/4D$ ~25 ms, which reflects an average arrival time of a molecule at this distance. The amperometric currents represent effectively the distributions of molecule arrival times at a given electrode for the specific event. The spike starting time reflects the arrival of the first molecules. (*Inset*) The determination of spike starting time for this event, which lags behind the time of release by ~1 ms. The longest delay between release and spike starting time was ~3 ms. *A* shows that the spike starting time of the smallest spike (green trace) is ~10 ms but this distance is nearly twice the distance between a release event near the center and an electrode. The delay of the green trace is thus approximately four times longer than the maximal delay for an event near the center, consistent with the 3-ms maximum delay we found in our analysis. (*C*) The contour graph showing the root of the sum of squared deviations between measured and simulated charge ratios measured by the different electrodes as a function of *x* and *y* positions. The deviation at the determined releasing site (red mark) of the example ECD event is 0.003.

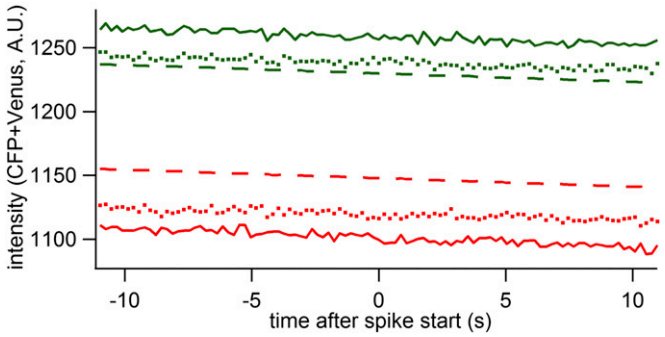


**Fig. S2.** Average time course of total fluorescence (YFP+CFP) in the central 4 pixels (solid lines), the peripheral 20 pixels of the six-by-six-pixel area (dotted lines), and averaged over the whole footprint of the cells (dashed lines) for non-AFS events (green lines) and AFS events (red lines).

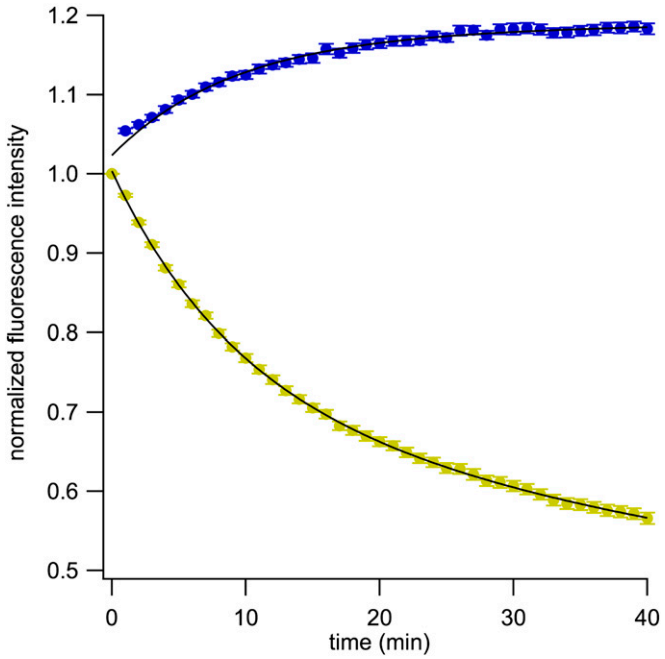


**Fig. S3.** Acceptor photobleaching of SCORE in live chromaffin cells leads to an increase of fluorescence intensity in the CFP channel (blue line) and a decrease in the YFP channel (yellow line). The continuous lines are double exponential fits to the respective intensity time courses. Normalized intensities were averaged from 19 experiments.

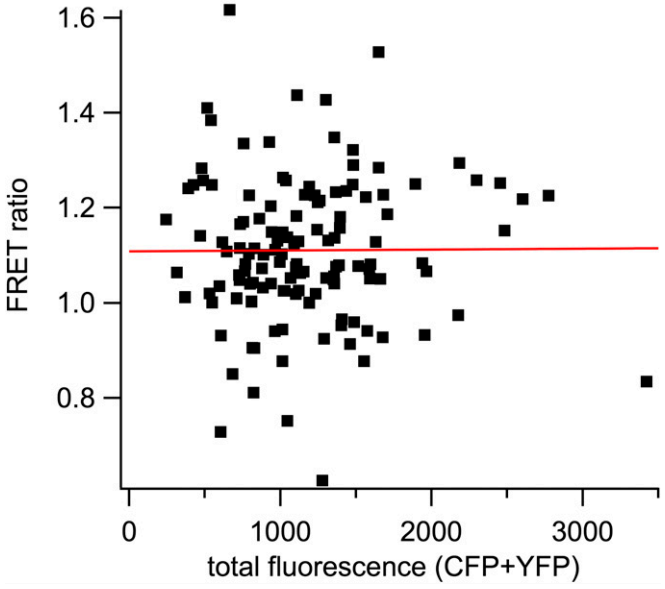


**Fig. S4.** FRET ratio in the footprint of individual cells plotted versus total fluorescence as a measure of expression level. Linear regression yielded a slope of $0 \pm 3 \times 10^{-6}$.

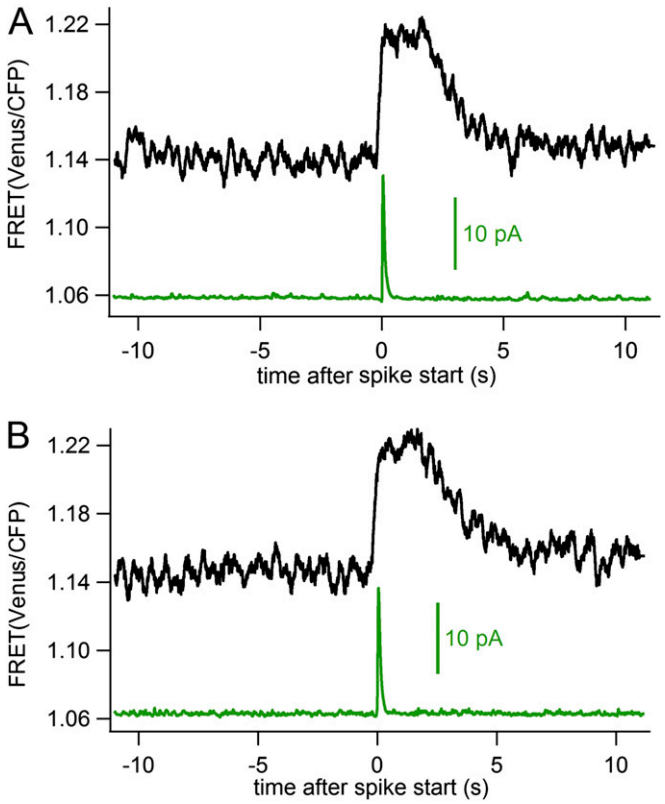


**Fig. S5.** Averaged time course of FRET signals (black line) obtained with the event correlation microscopy (ECOM) method. Traces were aligned at amperometric spike starting time (green line) (time 0). (*A*) ECOM average from 903 amperometric spikes with no detectable foot signal (non-AFS events). (*B*) ECOM average from 581 amperometric spikes that showed a detectable foot signal (AFS events).

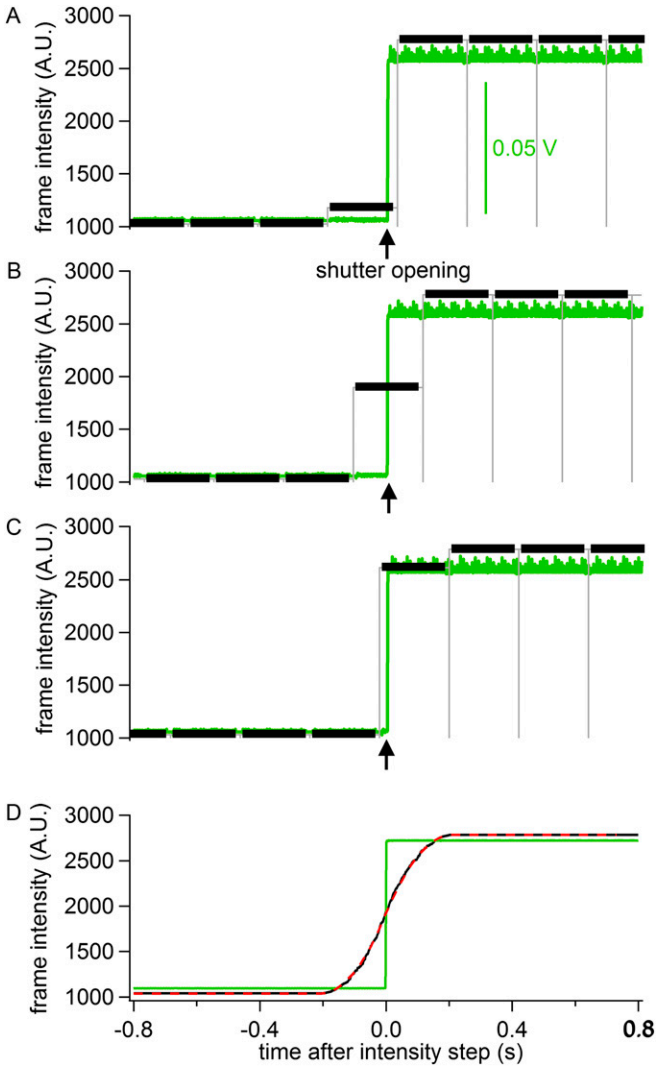


**Fig. S6.** ECOM method illustrated with photodiode recording of intensity step. **(***A*–*C***)** Shutter opening (arrows) produces step intensity change and stepwise photodiode response (green line). Image frame times are indicated by vertical gray lines and include 200-ms exposure time (black horizontal bars) and 19-ms interframe interval. Traces were temporally aligned at time of photodiode response step. Brightness of transition frame depends on time of shutter opening during the frame. (*D*) Averaged time course of photocurrent (green) and normalized image brightness (black line) from 262 shutter openings shows 50% rise time at time −0.05 ± 0.08 ms. The black curve was fitted well with the step response function (Eq. **1**) of image brightness (dashed red line).

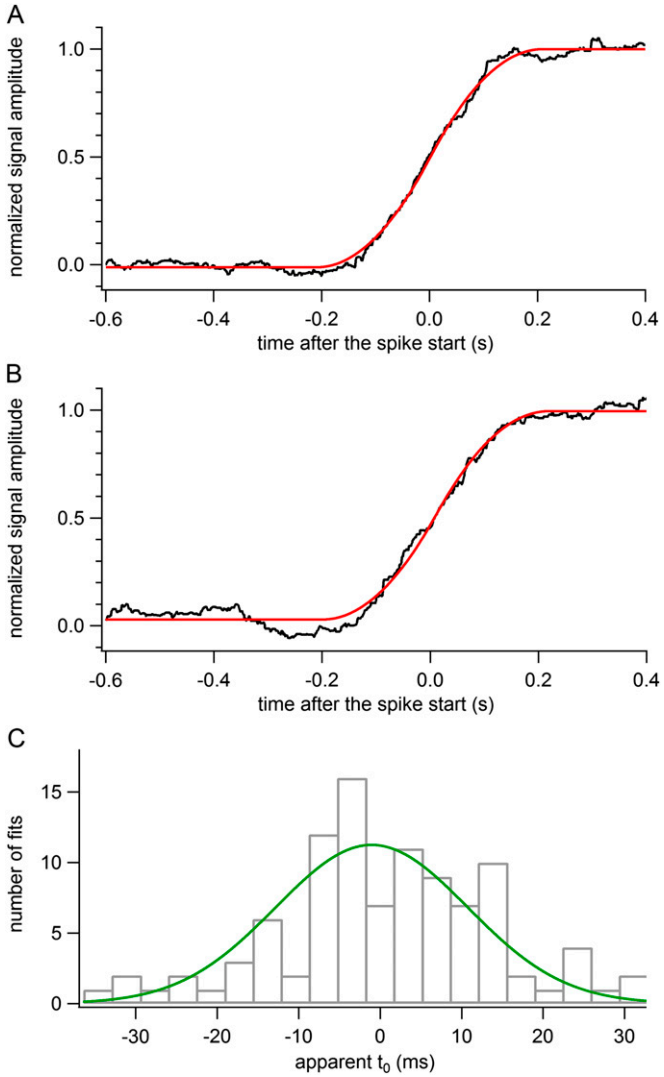


**Fig. S7.** Timing precision obtained by ECOM method with signal-to-noise ratio (SNR) of 20. (*A* and *B*) Two examples of ECOM averages of 100 simulated signals (black traces) with a SNR of 2 giving an SNR of 20 in the average, fitted (red lines) in the same way as the experimental data. The fitted $t_0$ values were 0 and +9 ms for traces in *A* and *B*, respectively. (*C*) Distribution of apparent $t_0$ values (bars) obtained from fitting 100 averages of 100 individual signals like those in *A* and *B*. The Gaussian fit yields a peak at −1 ± 2 ms and a SD of 12 ms.

**Table S1. Quantification of the fluorescence intensities of CFP+Venus channels, FRET ratio before fusion (pre-FRET ratio), and FRET ratio change at the release sites and control regions (footprint circle) for non-AFS and AFS events**

| Fluorescence parameter | Non-AFS sites vs. control (footprint) | AFS sites vs. control (footprint) |
|---|---|---|
| CFP+Venus, a.u. | 1,262 ± 33 ($n$ = 903) vs. 1,231 ± 25 ($n$ = 903) | 1,105 ± 24 ($n$ = 581) vs. 1,151 ± 28 ($n$ = 581) |
| Pre-FRET ratio (Venus/CFP) | 1.1409 ± 0.0074 vs. 1.1128 ± 0.0058 | 1.1458 ± 0.0065 vs. 1.1172 ± 0.0071 |
| FRET ratio change | 0.0718 ± 0.0019 vs. −0.0005 ± 0.0018 | 0.0719 ± 0.0020 vs. −0.0005 ± 0.0022 |